Supplementary Information for Characterization of Diarylethene-Based Photoswitches with Core and Valence Photoabsorption and Photoemission Spectroscopies

M. Pini[1], S. Severino[1], L. Mai[1], L. Colaizzi[1], M. Alagia[2], O. Plekan[3], R. Richter[3,a], E. Arfaoui[4], F. Montorsi[4], F. Segatta[4], M. Garavelli[4], S. R. Aloïse[5], L. Poisson[6] R. Borrego-Varillas[7], M. Lucchini[1,7], M. Coreno[2,8], M. Nisoli[1,7], M. Reduzzi[1,*], A. Nenov[3,*]

[1] Politecnico di Milano, Physics Department, Piazza Leonardo da Vinci 32, 20133, Milan, Italy
[2] CNR - Istituto Officina dei Materiali (IOM), Laboratorio TASC, Area Science Park Basovizza, Trieste, Italy
[3] Elettra-Sincrotrone Trieste, Strada Statale 14 - km 163.5, in AREA Science Park, IT-34149 Basovizza, Trieste, Italy
[4] Universitá di Bologna - Alma Mater Studiorum, Dipartimento di Chimica Industriale “Toso Montanari", Via Piero Gobetti 85, 40129 - Bologna, Italy
[5] LASIRE - Laboratoire de Spectroscopie pour les Interactions, la Réactivité et l’Environnement, Université de Lille, CNRS, UMR 8516, 59500 Lille, France
[6]Université Paris-Saclay, ISMO, CNRS, Rue André Rivière, 91400 Orsay, France
[7] CNR, Istituto di Fotonica e Nanotecnologie, Piazza Leonardo da Vinci 32, 20133, Milan, Italy
[8] ISM-CNR, Instituto di Struttura della Materia, LD2 Unit, 34149 Trieste, Italy
∗corresponding authors: artur.nenov@unibo.it maurizio.reduzzi@polimi.it, *a* deceased

Mass spectra

Only the mass spectrum of BTF6 was recorded: it is plotted in Figure S1, while Table 1 summarizes the tentative assignment of the most prominent peaks.

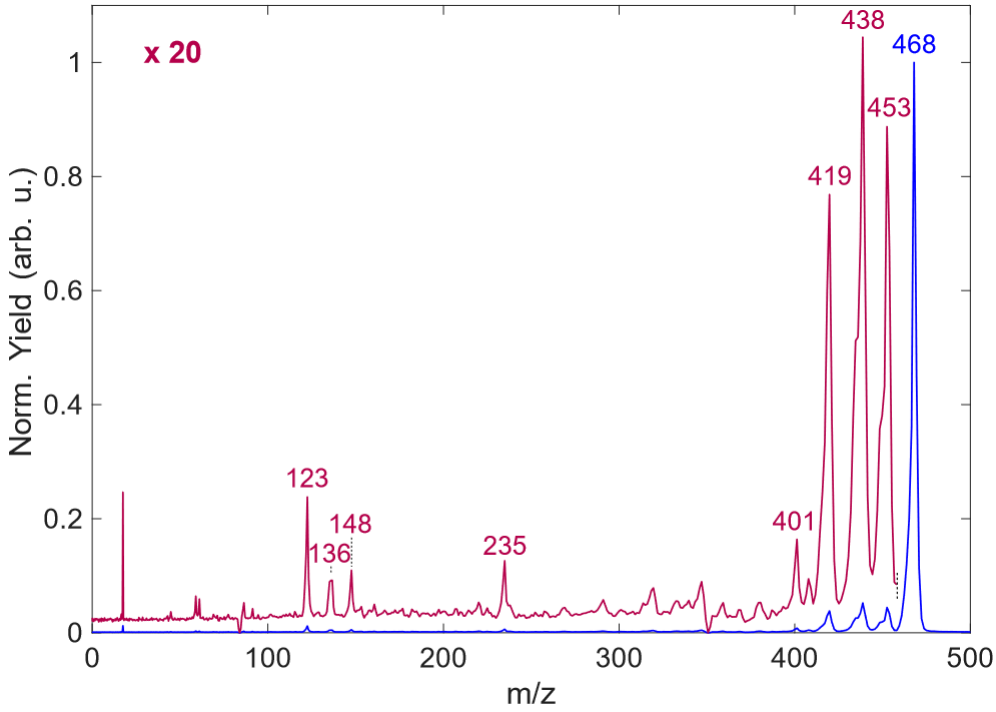

Figure S1: The recorded mass spectrum for BTF6 (blue), overlaid with its 20x magnification (red), where the parent ion (m/z = 468) is not shown to highlight the lighter fragments. The m/z of the most prominent peaks is reported above them.

BTF6 - Mass Spectrum

m/z	Assignment
468	(parent ion) M^+
453	$(M - CH_3)^+$
438	$(M - 2CH_3)^+$
419	$(M - 2CH_3 - F)^+$
401	$(M - 2CH_3 - 2F)^+$
235	(dication) M^{2+}
148	$C_8H_5SCH_3^+$
136	$C_8H_5S^+$
123	unidentified

Table 1: Tentative assignment for the most prominent peaks of BTF6 mass spectrum.

Geometries

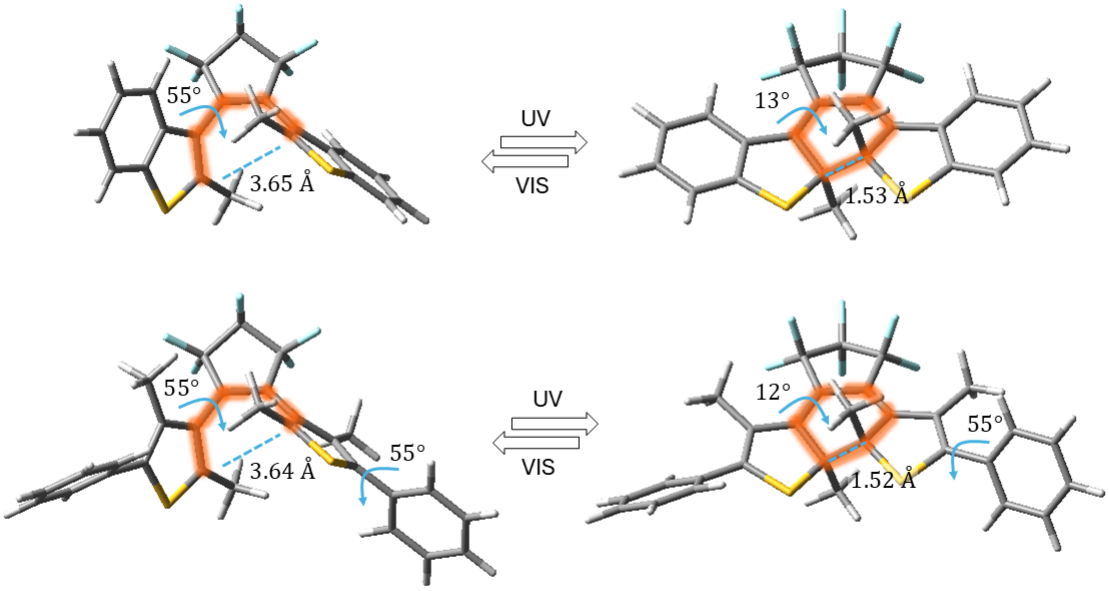

Figure S2: 3D structures of the target molecules (top) BTF6 (parallel conformation) and (bottom) PTF6 in their open-ring (OR) and closed-ring (CR) forms, highlighting hexatriene/cyclohexadiene units involved in the electrocyclic reaction as well as the values of several representative degrees of freedom.

Geometries

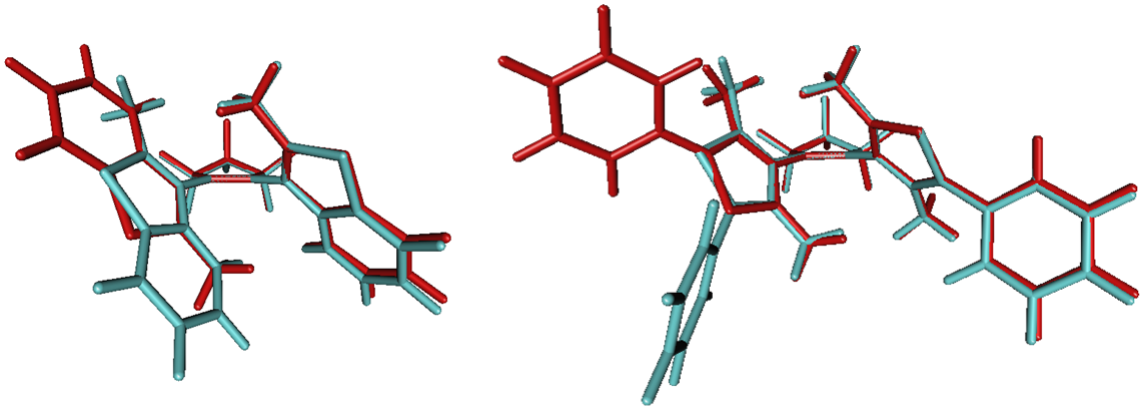

Figure S3: Comparison of the structures of the parallel (cyan) and anti-parallel (red) OR forms of BTF6 (left) and PTF6 (right).

Computational details

Active space definition for XPS and NEXAFS

Core-ionizations and -excitations are realized within the core-valence separation (CVS) approximations. By means of a projection technique all configuration state functions with a maximum

occupation of the core orbitals are eliminated from the configurational space. [1]. The AS includes the core orbital(s) of a single atom (1s orbital for carbons, a set of three 2p orbitals for sulfurs) placed in the sub-space RAS1 and kept frozen. A Cholesky localization scheme is used to localize core orbitals on single atomic sites [2]. The use of single atomic sites in the calculations is a common strategy adopted with other levels of theory [3] which streamlines post-processing and analysis. Whereas it neglects possible mixing of core-states involving different atoms, it is justified by the generally excellent agreement between theory and experiment indicating that the mixing is weak. The active space is completed by a set of valence occupied and virtual orbitals - usually of π-nature - distributed between sub-spaces RAS2 and RAS3, respectively, aimed at improving the description of electron correlation. In order to limit the computational cost we allow for up to four intra-valence excitations.

For BTF6 we use RAS(15,1,4;1,7,7) and RAS(19,1,4;3,7,7) for XPS simulations at the carbon K-edge and at the sulfur $L_{2,3}$-edge, respectively. In analogy, for PTF6 we use RAS(19,1,4;1,9,9) and RAS(23,1,4;3,9,9). Thereby, the valence orbital sets are comprised entirely of π molecular orbitals. Only a single core-ionized state was computed for each carbon atom whereas state-averaging over three core-ionized states was performed for the sulfur. Tests with reduced valence sub-spaces, containing only 10 valence orbitals (i.e. 5 occupied and 5 virtual) were carried out at the sulfur $L_{2,3}$-edge, demonstrating that the computational cost can be significantly lowered without sacrificing accuracy.

Specific to NEXAFS spectroscopy, the composition of the sub-space of virtual orbitals (i.e. RAS3) determines the nature of the core-excited states (i.e. core-to-π^*, core-to-σ^*, core-to-Rydberg) and the completeness of the spectrum. Different strategies were pursued for the carbon K-edge and the sulfur $L_{2,3}$-edge, dictated by the angular momentum selection rule in atomic spectroscopy $\Delta l = \pm 1$ which (loosely) determines signal intensities in core-excited spectra of molecules.

Specifically, the most intense contributions in the carbon pre-edge spectrum arise from transitions to π^* orbitals (exhibiting large MO coefficients from $2p$ atomic orbitals). Low intensity contributions arise due to transitions in virtual orbitals of (pseudo) Rydberg- and σ^*-type. Thus, a two-step strategy was adopted. In the first step, SA-10-RAS(16,1,4;1,7,7) and SA-10-RAS(20,1,4;1,9,9) for BTF6 and PTF6, respectively, comprised entirely of π molecular orbitals were used to describe accurately core-to-π^* transitions and shake-up satellites, i.e., less intense features in the spectra arising from mixed double excitations in which a core-excitation is accompanied by a valence π-to-π^* transition. Subsequently, the π and π^* orbitals were rotated out of the AS and replaced with a set of 10 virtual orbitals, which results in a SA-10-RAS(2,1,1;1,0,10) for both BTF6 and PTF6 and targets a qualitative description of core-to-Rydberg and core-to-σ^* transitions.

Instead, according to the selection rule the most intense contributions in the sulfur $L_{2,3}$ pre-edge spectrum arise from transitions to orbitals with $4s$- and $3d$-character on the sulfur. Core-to-π^* transitions are, indeed, present in the pre-edge region but are an order of magnitude less intense. Since a full-π AS extended with additional orbitals of s/d-type is unfeasible, trials were carried out to determine the optimal reduced AS which allows to capture the main contributions. The optimal AS compositions were found to be SA-25-CAS(6,11) and SA-19-CAS(6,9) for BTF6 and PTF6, respectively, containing four virtual orbitals with dominant s/d-character and additional four (BTF6) / two (PTF6) virtual orbitals of π^*-character, which have a negligible contribution to the spectra but confer active space stability. The number of states in the state-averaging was determined considering the electronic ground state and an excitation out of each of the three 2p core orbitals into each virtual orbital. The minimal AS (CAS(6,11) and CAS(6,9)) calculations presented convergence problems in the CASPT2 correction of the electronic ground state, presumably due to near-degenerate configurations involving occupied π-orbitals left outside of the minimal AS. For this reason, no reliable theoretical ground state reference could be obtained for calculating the relative energies of the core-excited states. Hence, for both systems the NEXAFS spectra were simulated considering only the (absolute) core-excited states energies and the resulting spectra were shifted to make the first peak coincide with its experimental counterpart.

Active space definition for PES

The active space comprises of valence occupied and virtual orbitals of π-nature, distributed between sub-spaces RAS1 and RAS3 (thus leaving RAS2 empty) and allowing for up to four holes and four excitations, respectively. A total of 8 and 10 valence-ionized states were computed in the case of BTF6 and PTF6, respectively, giving rise to SA-8-RASSCF(13,4,4;7,0,7) and SA-10-RASSCF(17,4,4;9,0,9). A different strategy was followed to account for ionization from σ-orbitals. The AS comprised of 20 orbitals with π and σ character, with no virtual orbitals included, leading to a SA-20-CAS(39,20) (i.e. 39 electrons in 20 orbitals). This minimal AS allows to optimize the form of the lowest 20 occupied orbitals subject to ionization but lacks the flexibility to describe electron correlation effects. As a consequence the error with respect to the experimental data (which translates into a rigid shift in the simulated spectrum) is in the order of 1 eV (compared to 0.5 eV correction applied in the case of full-π active spaces). Despite the larger absolute error, the results with CAS(39,20) are presented in the main text as they allow for a more complete description of the PES. The spectra obtained with the restricted AS are presented in Fig. S17.

Sulfur $L_{2,3}$-edge

XPS

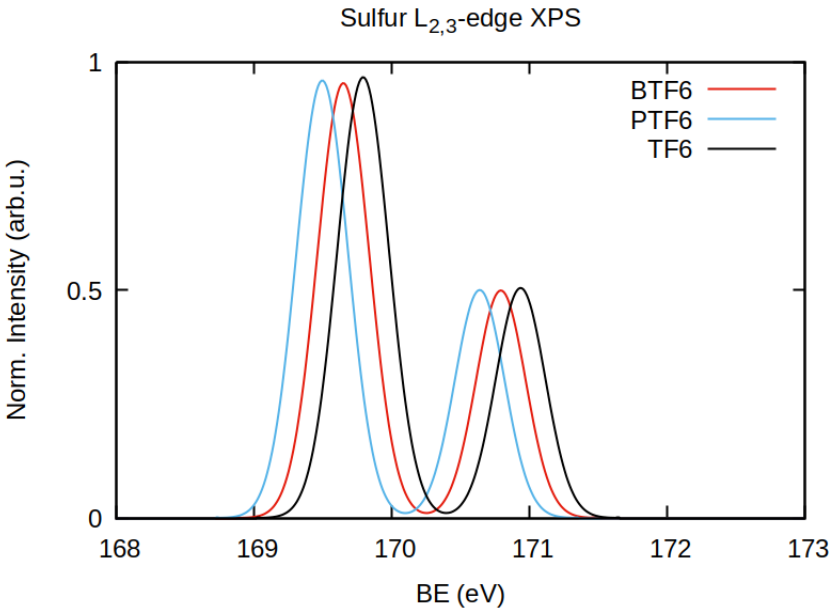

Figure S4: Comparison between the XPS spectra at the $L_{2,3}$ edge of sulfur for BTF6 (red), PTF6 (blue) and TF6 (black). As evident stripping the phenyl groups for PTF6 leads to a blue-shift of the signal due to the reduced extension of the conjugation.

NEXAFS

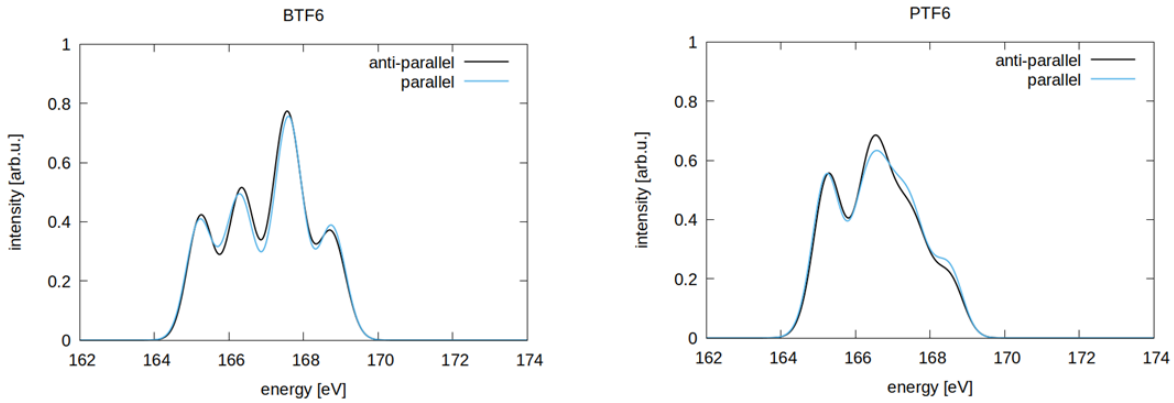

Figure S5: Comparison of the NEXAFS spectra at the sulfur $L_{2,3}$-edge of the parallel (blue) and anti-parallel (black) OR forms of BTF6 (left) and PTF6 (right) computed at the SS-PT2/SA-25-CAS(6,11) and SS-PT2/SA-19-CAS(6,9) levels of theory, respectively.

Carbon K-edge

NEXAFS

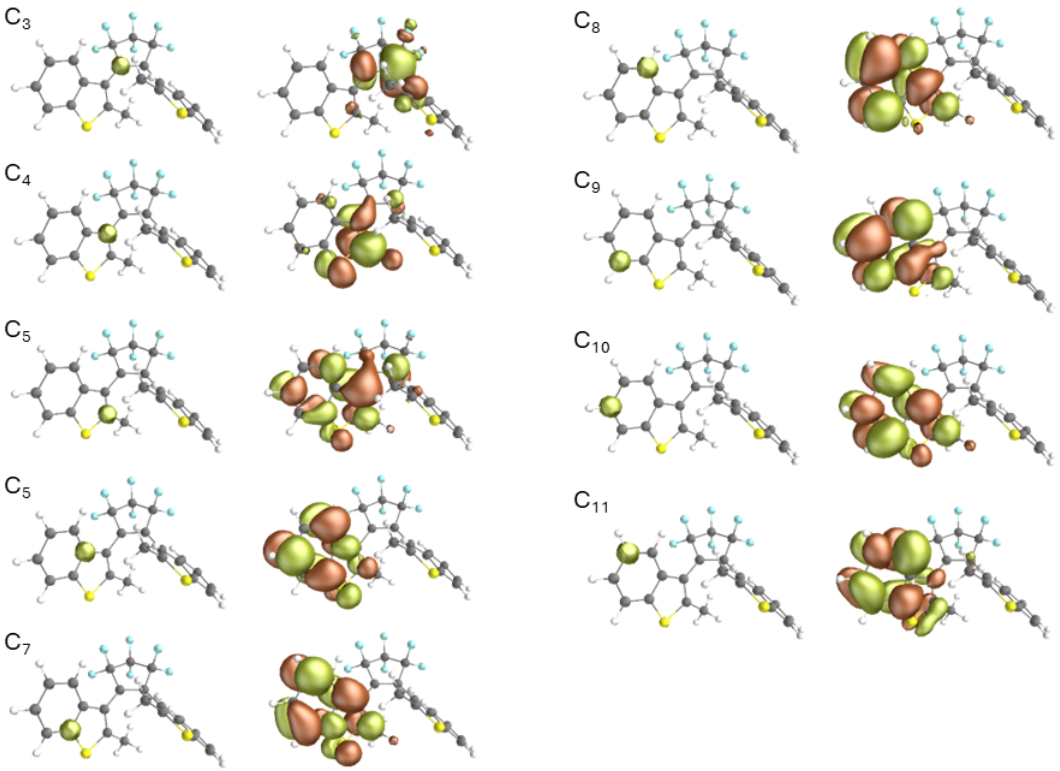

Figure S6: Pairs of 1s core and corresponding relaxed LUMO giving rise to 284.0-286.0 eV signal at the carbon K-edge for the anti-parallel conformation of BTF6. C_1, C_2 and the methyl carbon are omitted as they do not contribute a bright peak in the NEXAFS.

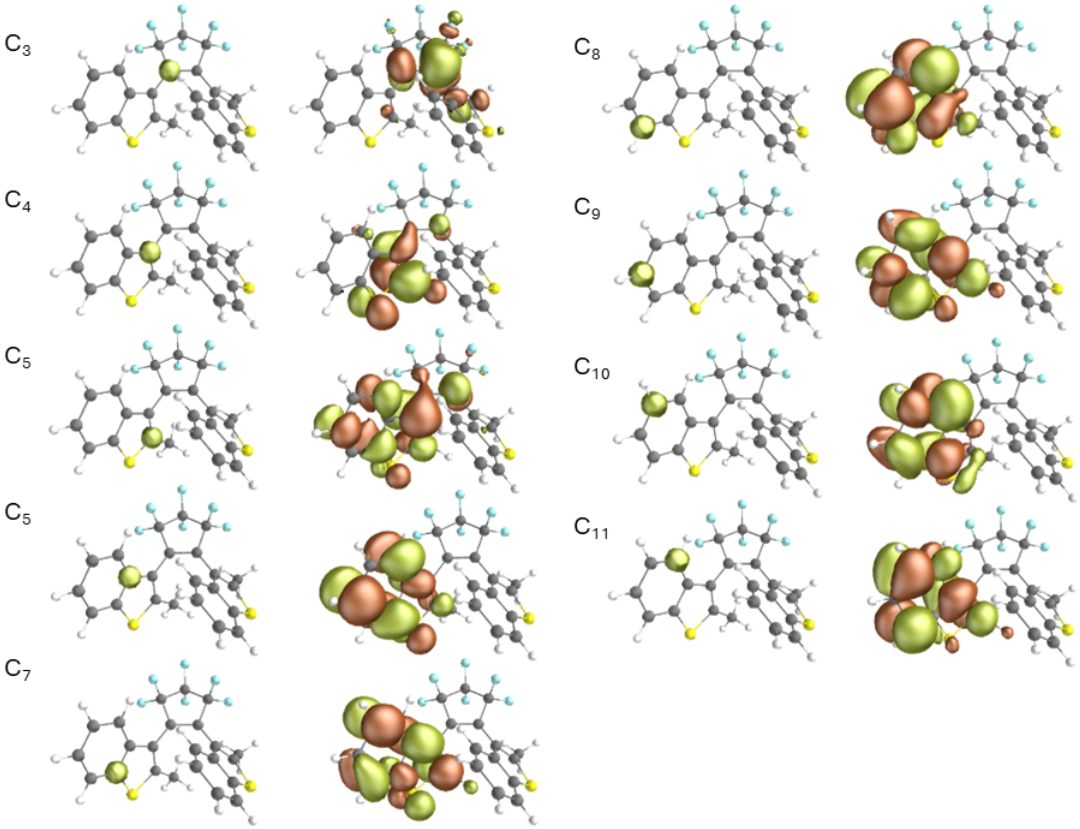

Figure S7: Pairs of 1s core and corresponding relaxed LUMO giving rise to 284.0-286.0 eV signal at the carbon K-edge for the parallel conformation of BTF6. C_1, C_2 and the methyl carbon are omitted as they do not contribute a bright peak in the NEXAFS.

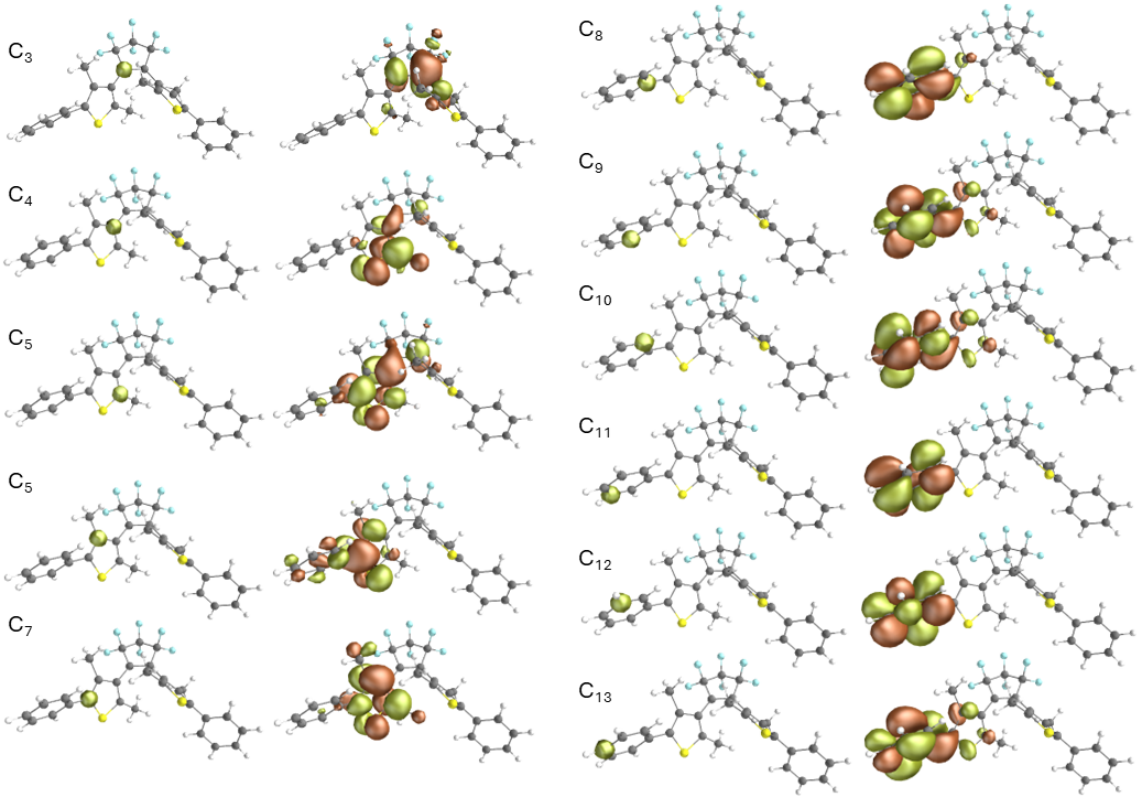

Figure S8: Pairs of 1s core and corresponding relaxed LUMO giving rise to 284.0-286.0 eV signal at the carbon K-edge for the anti-parallel conformation of PTF6. C_1, C_2 and the methyl carbons are omitted as they do not contribute a bright peak in the NEXAFS.

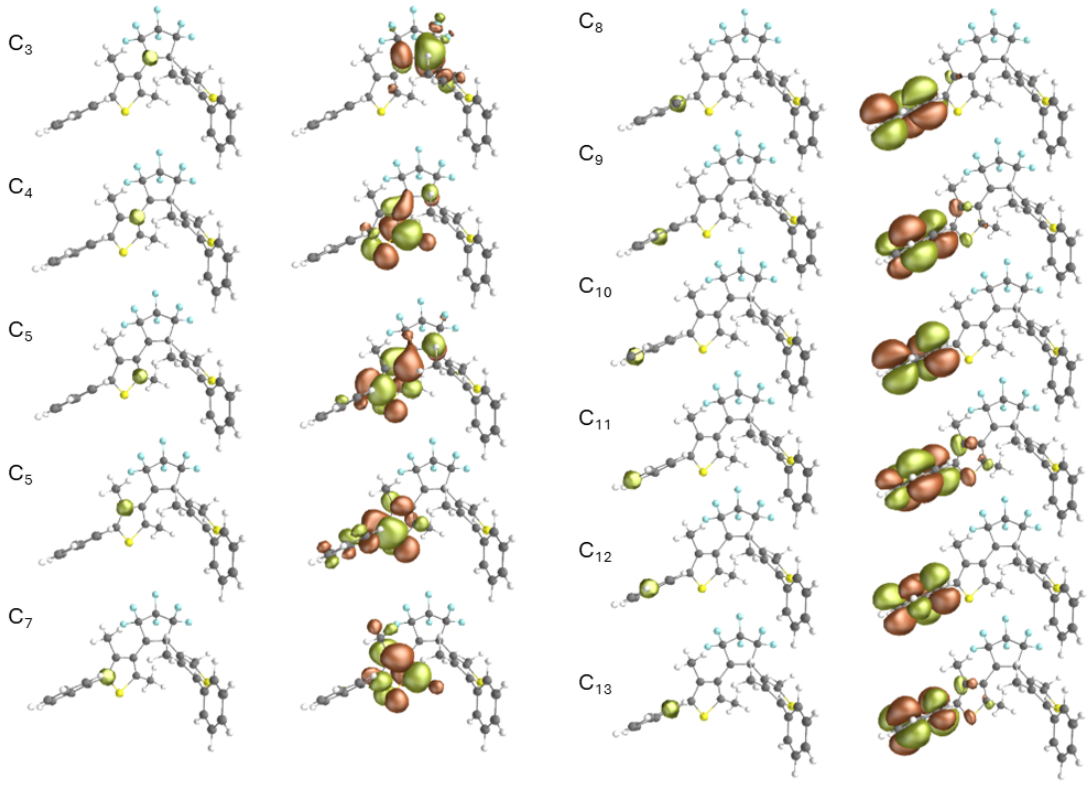

Figure S9: Pairs of 1s core and corresponding relaxed LUMO giving rise to 284.0-286.0 eV signal at the carbon K-edge for the parallel conformation of PTF6. C_1, C_2 and the methyl carbons are omitted as they do not contribute a bright peak in the NEXAFS.

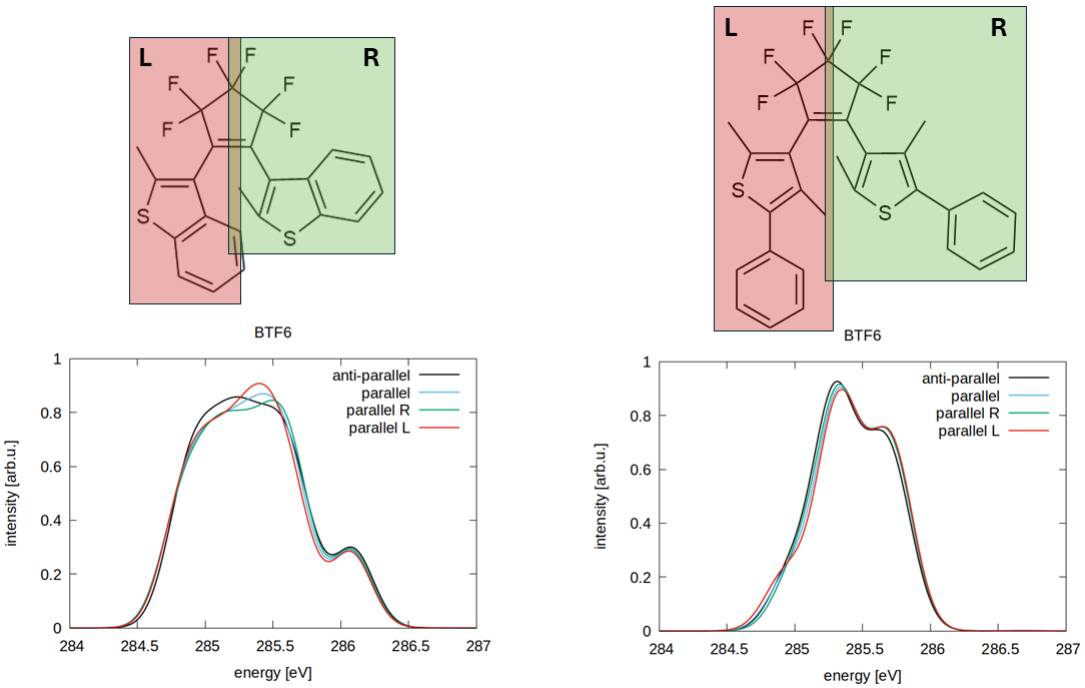

Figure S10: Comparison of the NEXAFS spectra at the carbon K-edge of the parallel (blue) and anti-parallel (black) OR forms of BTF6 (left) and PTF6 (right) computed at the SS-PT2/SA-10-RAS(16,1,4;1,7,7) and SS-PT2/SA-10-RAS(20,1,4;1,9,9) levels of theory, respectively. Only contribution to the first transition 1s $\rightarrow \pi^*$ is shown. For the parallel form spectra obtained by considering only the left (L, red) or right (R, green) part of the molecule are also shown.

carbon #	BTF6 anti-parallel R (eV)	BTF6 parallel R (eV)	BTF6 parallel L (eV)	BTF6 Δ (eV)	PTF6 anti-parallel R (eV)	PTF6 parallel R (eV)	PTF6 parallel L (eV)	PTF6 Δ (eV)
1	291.49	291.48	291.48	-	291.59	291.60	291.60	-
2	290.70	290.68	290.69	-0.01	290.78	290.80	290.75	0.05
3	284.83	284.79	284.80	-0.01	284.97	284.99	284.93	0.06
4	285.48	285.48	285.43	0.05	285.67	285.70	285.70	0.00
5	285.57	285.59	285.55	0.04	285.64	285.67	285.69	-0.02
6	285.71	285.68	285.68	0.00	285.75	285.74	285.76	-0.02
7	286.09	286.08	286.07	0.01	285.78	285.79	285.78	0.01
8	285.21	285.20	285.21	-0.01	285.56	285.56	285.57	-0.01
9	285.10	285.09	285.09	0.00	285.28	285.31	285.32	-0.01
10	285.32	285.34	285.35	-0.01	285.33	285.33	285.36	-0.03
11	284.96	284.97	284.96	0.01	285.22	285.23	285.24	-0.01
12	-	-	-	-	285.35	285.37	285.37	0.00
13	-	-	-	-	285.27	285.29	285.29	0.00
$CH_3$1	286.49	286.57	286.64	-0.07	286.62	286.64	286.82	-0.18
$CH_3$2	-	-	-	-	286.71	286.72	286.53	0.19

Table 2: Core-excitation energies of the parallel and anti-parallel OR forms of BTF6 and PTF6 and relative difference Δ computed at the SS-PT2/SA-10-RAS(16,1,4;1,7,7) and SS-PT2/SA-10-RAS(20,1,4;1,9,9) levels of theory, respectively. For the parallel form values for "equivalent" atoms from the right (R) and left (L) part of the molecule are compared.

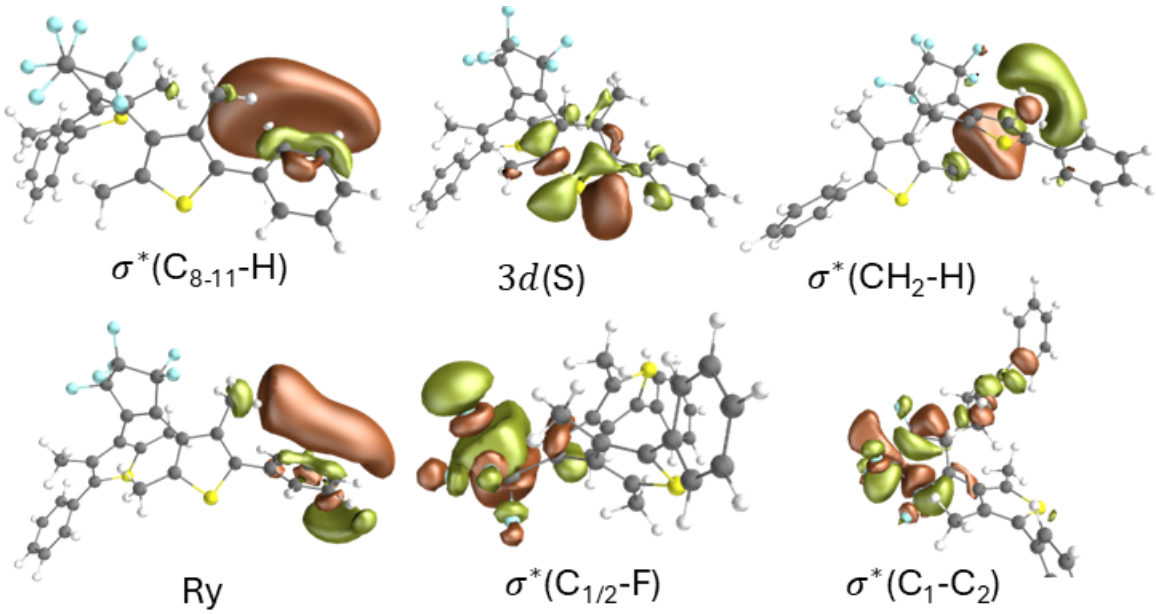

Figure S11: Representative arrival orbitals giving rise to signal above 286.0 eV at the carbon K-edge for the anti-parallel conformation of PTF6.

83

PES

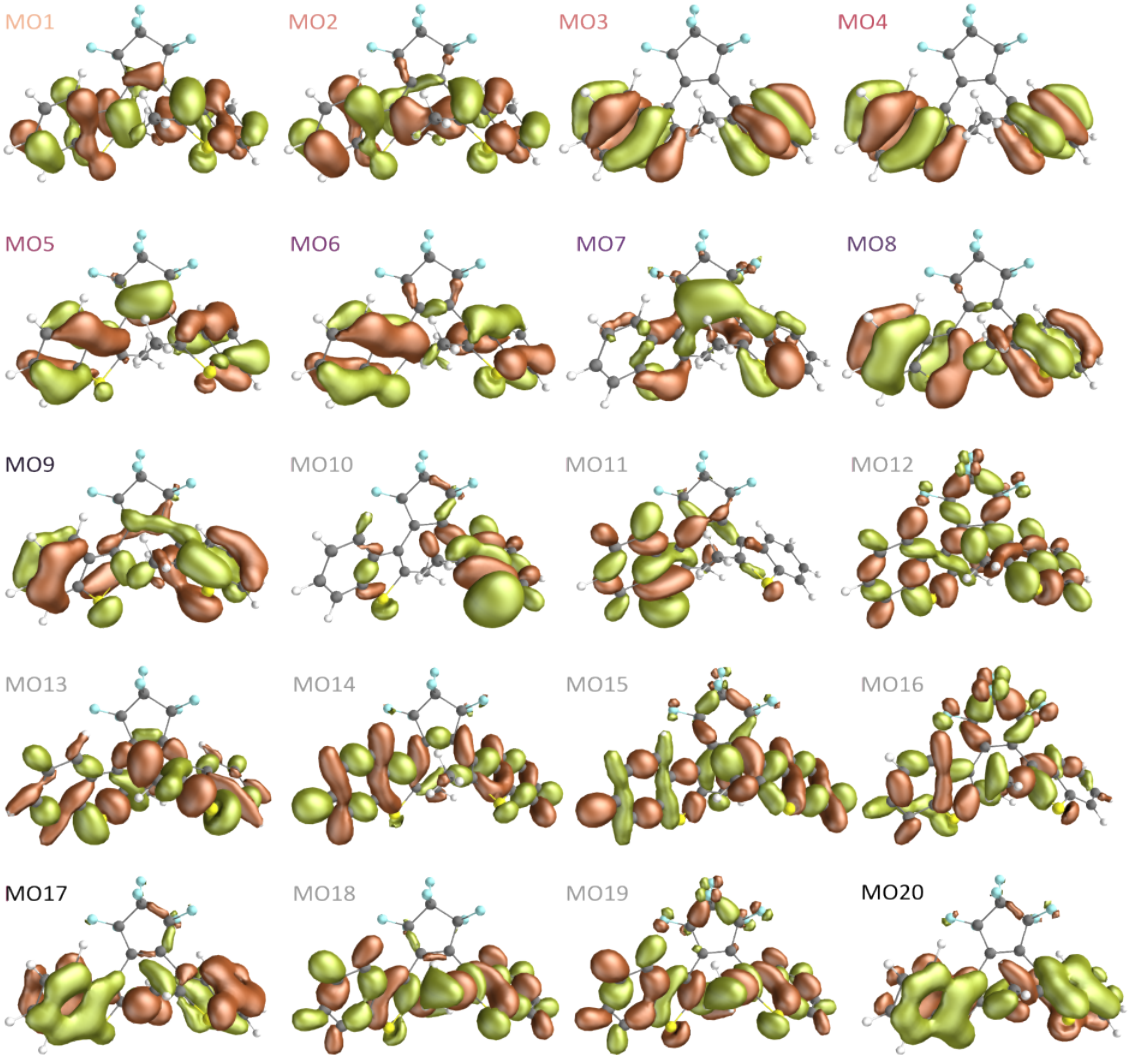

Figure S12: Active space occupied valence orbitals for anti-parallel conformation of BTF6. The color of each label is the same of the correspondent stick representing each contribution in the PES spectrum of the molecular system in panel (a) of Fig. 4 of the main text. The gray labels indicate orbitals with σ character, while colored labels describe orbitals having a π character.

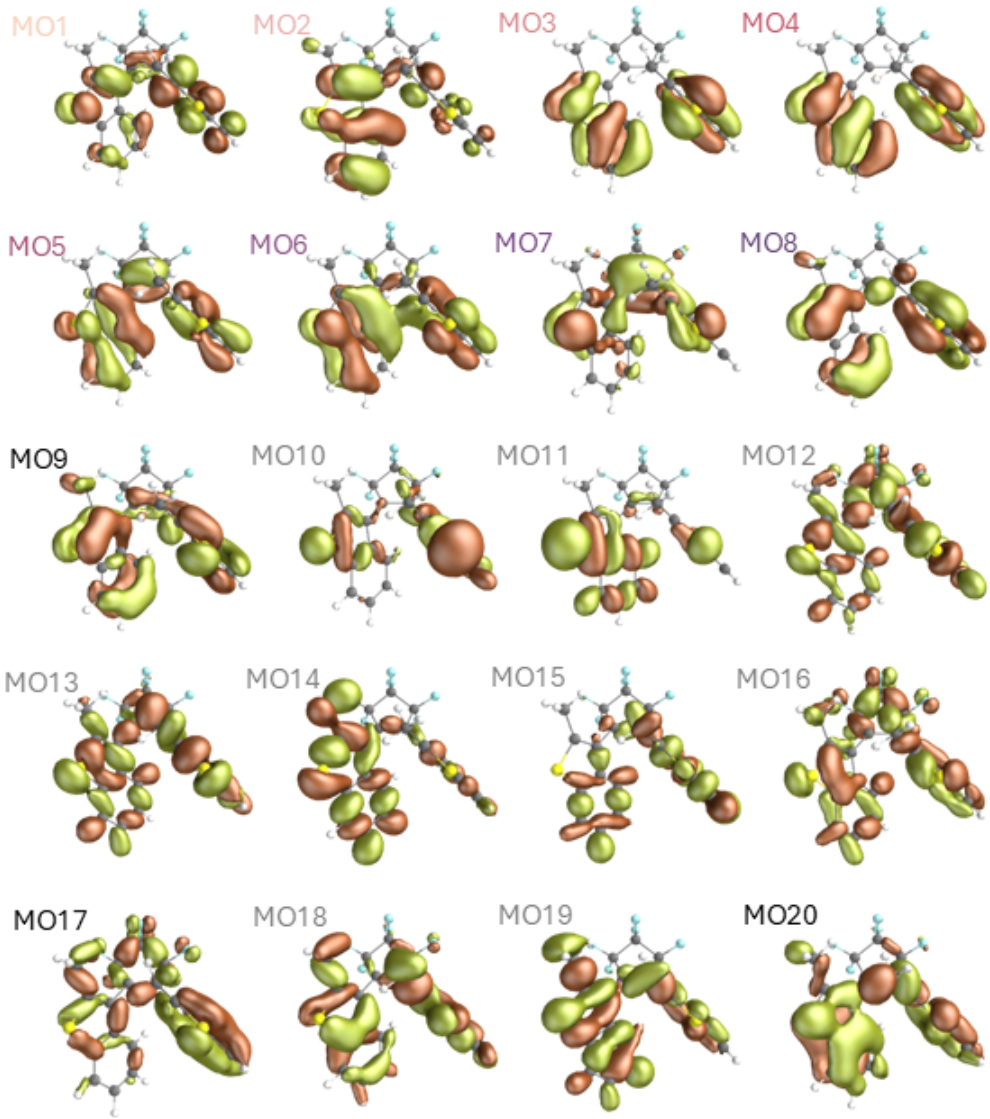

Figure S13: Active space occupied valence orbitals for parallel conformation of BTF6. The color of each label is the same of the correspondent stick representing each contribution in the PES spectrum of the molecular system in panel (a) of Fig. 4 of the main text. The gray labels indicate orbitals with σ character, while colored labels describe orbitals having a π character.

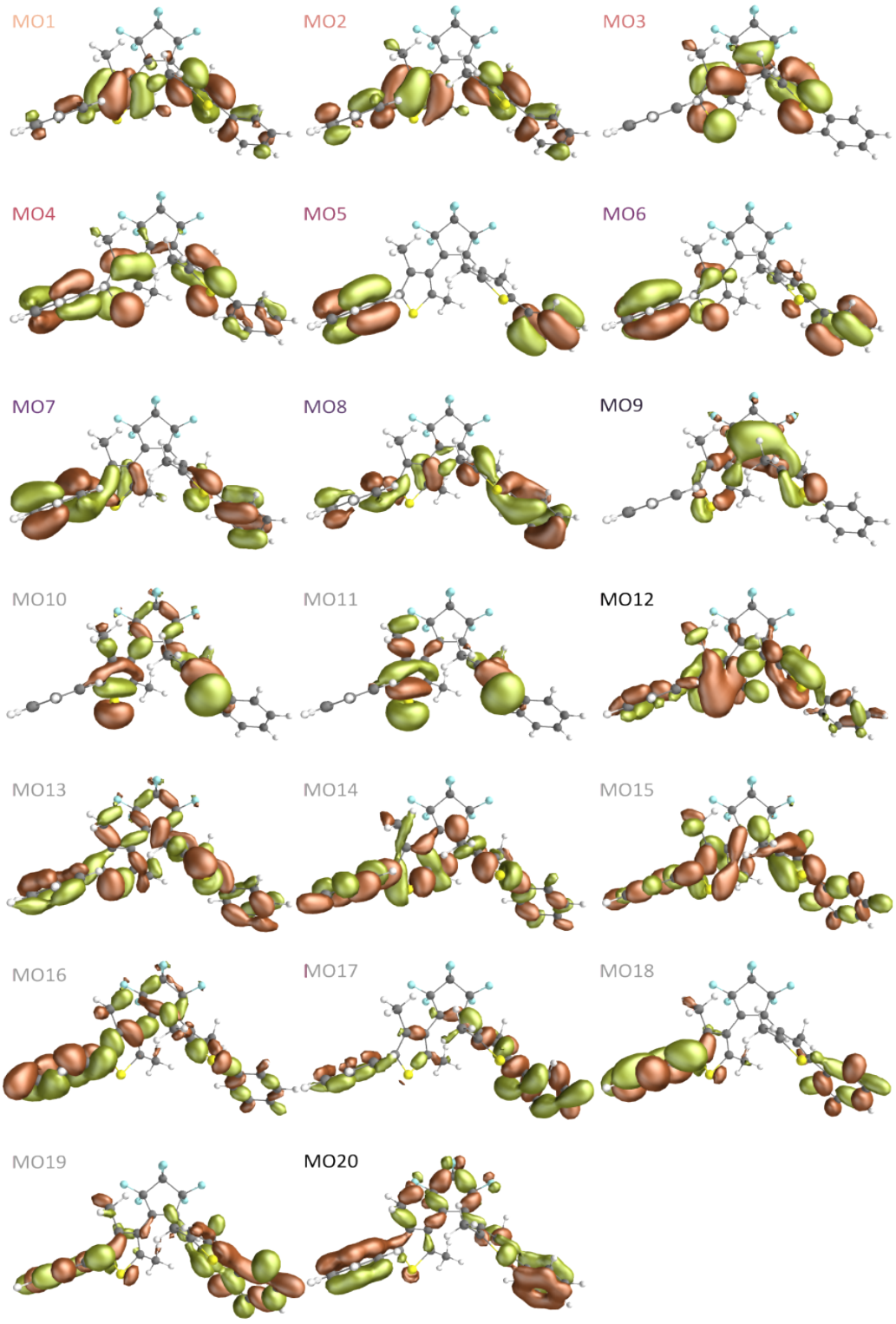

Figure S14: Active space occupied valence orbitals for anti-parallel conformation of PTF6. The color of each label is the same of the correspondent stick representing each contribution in the PES spectrum of the molecular system in panel (b) of Fig. 4 of the main text. The gray labels indicate orbitals with σ character, while colored labels describe orbitals having a π character.

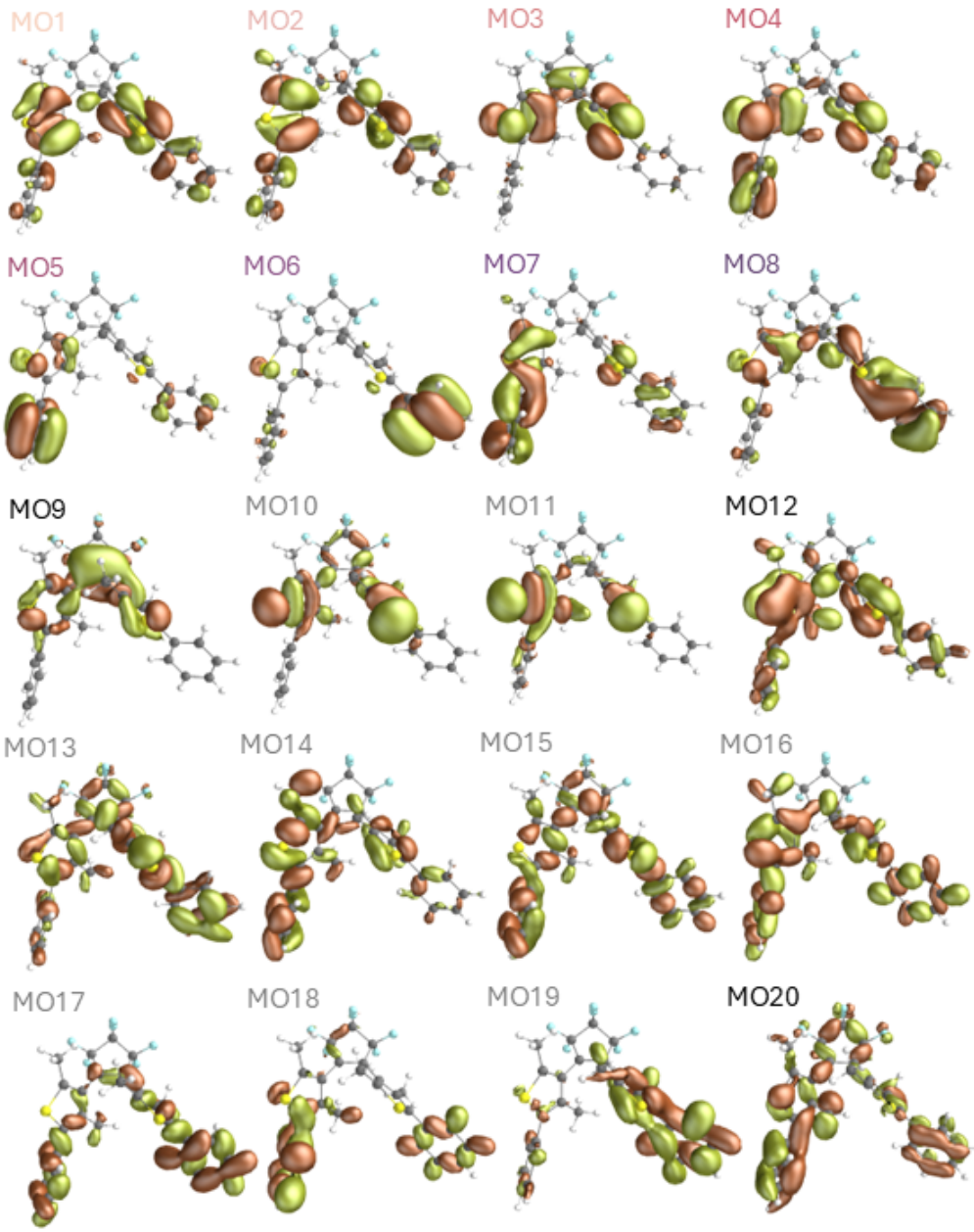

Figure S15: Active space occupied valence orbitals for parallel conformation of PTF6. The color of each label is the same of the correspondent stick representing each contribution in the PES spectrum of the molecular system in panel (b) of Fig. 4 of the main text. The gray labels indicate orbitals with σ character, while colored labels describe orbitals having a π character.

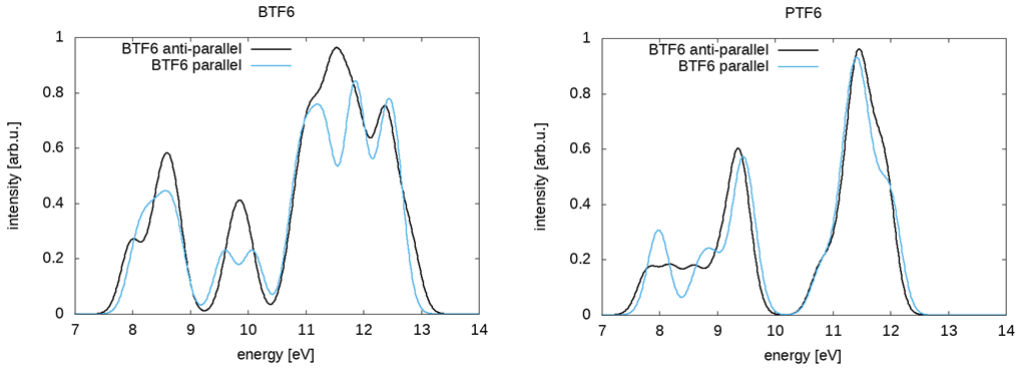

Figure S16: Comparison of the PES spectra of the parallel (blue) and anti-parallel (black) OR forms of BTF6 (left) and PTF6 (right) computed at the SS-PT2/SA-20-CAS(39,20) level of theory.

	BTF6			PTF6		
transition #	anti-parallel (eV)	parallel (eV)	Δ (eV)	anti-parallel (eV)	parallel (eV)	Δ (eV)
1	7.98	8.08	-0.10	7.80	7.94	-0.14
2	8.41	8.33	0.08	8.19	8.02	0.17
3	8.60	8.58	0.02	8.60	8.70	-0.10
4	8.74	8.77	-0.03	9.01	8.96	0.05
5	9.74	9.59	0.15	9.49	9.47	0.02
6	9.97	10.08	-0.11	9.33	9.59	0.26
7	10.81	10.79	0.02	9.30	9.40	-0.10
8	11.06	10.93	0.13	9.39	9.38	0.01
9	11.05	11.04	0.01	10.79	10.80	-0.01
10	11.45	11.34	0.11	11.10	11.13	-0.03
11	11.49	11.40	0.09	11.36	11.33	0.03
12	11.28	11.21	0.07	11.33	11.30	0.03
13	12.02	11.86	0.16	11.37	11.31	0.06
14	11.62	11.82	-0.20	11.50	11.52	-0.02
15	11.77	11.80	-0.03	11.49	11.45	0.04
16	11.88	12.00	-0.12	11.54	11.52	0.02
17	12.50	12.36	0.14	11.69	11.67	0.02
18	12.33	12.35	-0.02	11.94	11.86	0.08
19	12.35	12.55	-0.20	11.91	12.04	-0.13
20	12.80	12.56	0.24	11.88	12.02	-0.14

Table 3: Ionization energies of the parallel and anti-parallel OR forms of BTF6 and PTF6 and relative difference Δ computed at the SS-PT2/SA-20-CAS(39,20) level of theory.

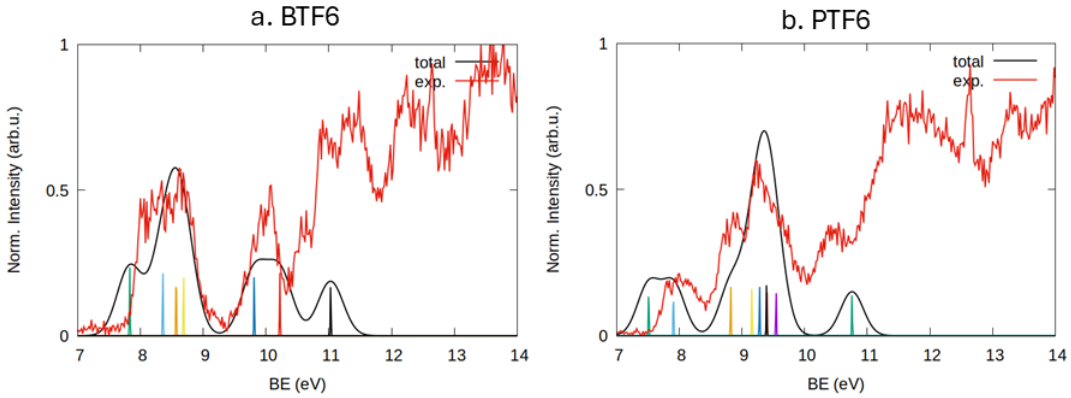

Figure S17: PES spectra of the OR(ap) form of BTF6 (a) and PTF6 (b) obtained with the full-π active spaces SA-8-RASSCF(13,4,4;7,0,7) and SA-10-RASSCF(17,4,4;9,0,9), respectively. Computed signals have been blue-shifted uniformly by 0.5 eV.

84

BTF6 Closed-ring form

XPS - Sulfur $L_{2,3}$-edge

	BE (eV)	Leading transition
S_1	169.05	
S_2	169.15	2p ionization
S_3	170.24	

Table 4: Theoretically calculated sulfur $L_{2,3}$-edge binding energies of the CR form of BTF6, with the inclusion of spin-orbit-coupling. The reported binding energy values have been shifted by +0.05 eV as done for the OR form. The Dyson norm for all the ionization processes in the two molecules is equal to 1.50.

XPS - Carbon K-edge

Transition	BE (eV)	Dyson norm
C_1	296.08	0.72
C_2	295.93	0.72
C_3	290.65	0.57
C_4	290.56	0.60
C_5	291.53	0.72
C_6	290.58	0.65
C_7	290.80	0.63
C_8	290.28	0.64
C_9	290.23	0.59
C_{10}	290.15	0.57
C_{11}	290.21	0.61
$C(H_3)$	290.44	0.73

Table 5: Theoretically calculated carbon K-edge binding energies for the CR form of BTF6. BEs have been shifted by +0.25 eV as done for the OR form. The different signals contributing to the spectra are due to ionization from the core orbitals 1s of the C_i carbon atoms, with numeration reported in the first raw of Fig. 3 of the main paper.

NEXAFS - Carbon K-edge

Peak	Site	Energy (eV)	arrival MO
A	C_3	284.42	π^* LUMO
	C_4	284.18	
	C_6	284.73	
	C_7	285.16	
	C_8-C_{11}	284.38-284.85	

Table 6: Theoretically calculated core excited states at carbon K-edge of BTF6 and PTF6. For each carbon contributing to the NEXAFS signal and the transition energies are reported. Only transitions from carbons having oscillator strength larger than 10^{-4} are considered. No shift has been applied.

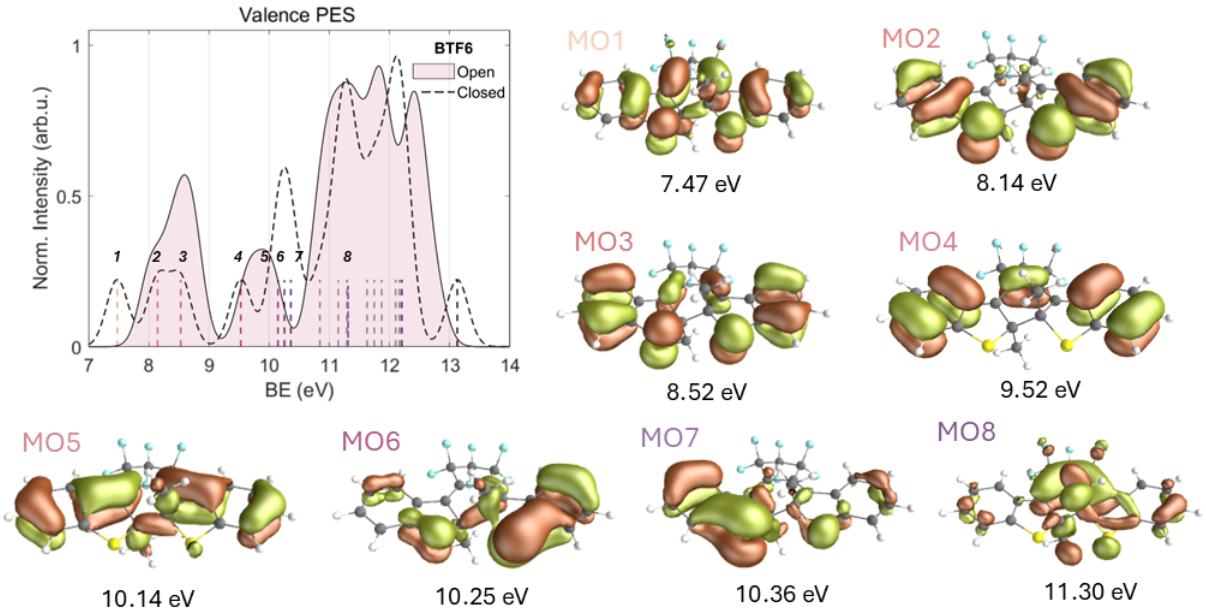

Figure S18: Simulated valence-ionization photoelectron spectra of the OR (shaded area) and CR (dashed line) form of BTF6, both shifted by +0.9 eV. Colored and gray lines stand for ionization from orbitals with and π and σ character, respectively. π MOs giving rise to the signal below 11 eV are shown.

References

[1] M. G. Delcey, L. Kragh Sørensen, M. Vacher, R. C. Couto, and M. Lundberg. Efficient calculations of a large number of highly excited states for multiconfigurational wavefunctions. *J. of Comput. Chem.*, 40(19):1789–1799, April 2019.

[2] F. Aquilante, T. Bondo Pedersen, A. Sánchez de Merás, and H. Koch. Fast noniterative orbital localization for large molecules. *J. Chem. Phys.*, 125(17):174101, November 2006.

[3] T. Fransson, I. E. Brumboiu, M. L. Vidal, P. Norman, S. Coriani, and A. Dreuw. XABOOM: An X-ray absorption benchmark of organic molecules based on carbon, nitrogen, and oxygen $1s \rightarrow \pi^*$ transitions. *Journal of Chemical Theory and Computation*, 17(3):1618–1637, 2021.